

Semi-spin-glass behavior in the Co_2TiO_4 compound

J. Hubsch

*Laboratoire de Minéralogie-Cristallographie,
Equipe de Recherche Associée No. 162 au Centre National de la Recherche Scientifique,
Université de Nancy I, B.P. 239, 54506 Vandoeuvre lès-Nancy Cédex, France*

G. Gavoille

*Laboratoire d'Electricité Automatique, Université de Nancy I,
B.P. 239, 54506 Vandoeuvre lès-Nancy Cédex, France*

(Received 13 April 1982)

Magnetic and neutron-diffraction measurements show that the magnetic ground state of the insulating spinel Co_2TiO_4 consists of a ferrimagnetic longitudinal component and of a spin-glass transverse component. Two transitions are observed, T_N for the ferrimagnetic component and T_G for the spin-glass component. The spin-glass behavior below T_G is discussed in detail and suggestions are made for the origin of the canting.

I. INTRODUCTION

We report on magnetic and neutron-diffraction measurements on the Co_2TiO_4 compound in which the nonmagnetic Ti^{4+} ions occupy the octahedral or B sites of the spinel structure. The Co^{2+} ions occupy the remaining B sites and the tetrahedral sites. At low temperature the spin configuration differs strongly from the Néel colinear structure observed in most of the magnetic compounds of spinel structure. The ground-state spin configuration is canted and a spin-glass-like behavior is observed along with a nonvanishing ferrimagnetic bulk magnetization. It is known that no long-range magnetic order takes place if the magnetic ions are so diluted that there is no percolation and spin-glass-like behavior is usually observed around the percolation threshold. For the B sites of the spinel structure the latter is 0.39,^{1,2} i.e., lower than the cobalt concentration. If similar compounds, Fe_2TiO_4 (Refs. 3–5) and Co_2SnO_4 (Refs. 6 and 7), certainly exhibit a spin-glass behavior it is not the case of $\text{Fe}_{1,4}\text{Mg}_{1,3}\text{Ti}_{0,3}\text{O}_4$ (Refs. 8–11) where the Fe^{3+} concentration on the B sites approaches 45%. One may then expect that Co_2TiO_4 is a highly frustrated system since frustration is known to lead to disordered ground-state spin configurations.^{12–19}

Several data reported here have been previously obtained by different authors^{20–22} and a good agreement has always been observed.

II. EXPERIMENTAL

The samples have been obtained by a ceramic method. Appropriate quantities of TiO_2 and CoO have been annealed at 1200°C and then ground. The procedure has been repeated several times. X-ray and neutron-diffraction patterns show an inverse spinel structure at room temperature. The lattice and oxygen parameters are, respectively, 8.45 \AA and 0.385 , and the reliability factor is 2.1% . The diffraction patterns do not depend on the rate of cooling of the samples and although the nuclear scattering factors of cobalt (0.25) and titanium (-0.335) are different no superlattice reflections are observed by neutron-diffraction experiments.

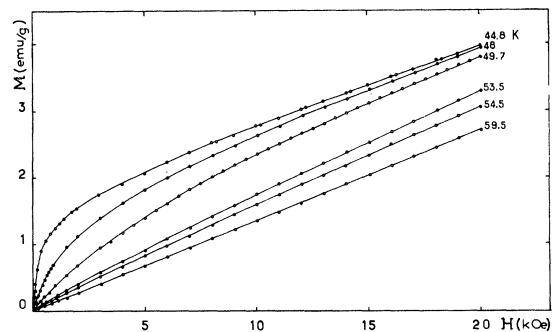


FIG. 1. Magnetization curves near the Néel temperature.

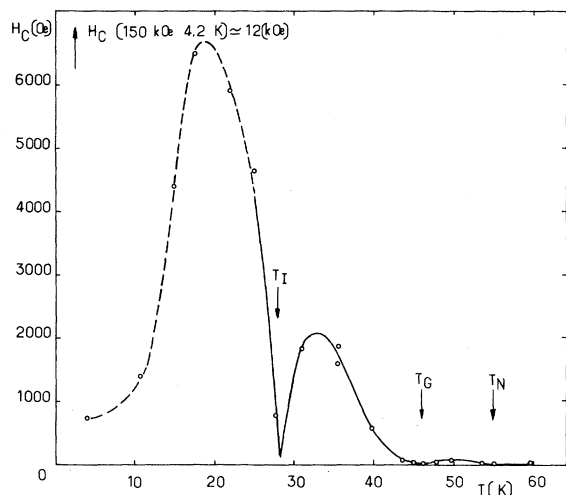


FIG. 2. Coercive field measured in 20-kOe field vs temperature. The arrows, respectively, indicate the compensation point T_I , the freezing temperature T_G , and the Néel temperature T_N .

We may consequently infer that there is no long-range order of the Ti ions on the B sites.

Most of the magnetic measurements have been carried out with a sample vibrating magnetometer in the temperature range 1.5–300 K and in fields up to 20 kOe. High-field magnetization curves have been obtained at the SNCI—Grenoble.

The neutron-diffraction patterns have been obtained at the Centre d'Etudes Nucléaires (CEN), Saclay, and at the Institut Laue Langevin (ILL), Grenoble, with respective neutron wavelengths of 1.14 and 2.43 Å.

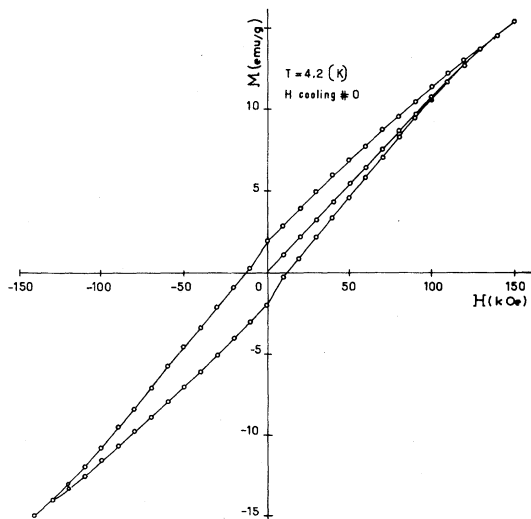


FIG. 3. High-field magnetization loop at 4.2 K.

III. RESULTS

A. Magnetic measurements

The magnetization M varies linearly with the magnetic field H above 55 K (Fig. 1) where the compound becomes paramagnetic. At high temperature the susceptibility follows a Curie-Weiss law, the Curie constant and temperature are, respectively, 5.7 emu/mole and -130 K, and the curvature of the reciprocal susceptibility above 55 K is typical of a ferrimagnetic. The magnetic moments of the Co^{2+} ions on the A and B sites are estimated from the gyromagnetic factors^{23–25}

$$g_A = 2.4, \quad g_B = 2.58,$$

respectively, as

$$m_A = 3.60\mu_B, \quad m_B = 3.87\mu_B.$$

This yields a Curie constant of 5.8 emu/mole in good agreement with the data. Between 46 and 55 K the magnetization curves (Fig. 1) are typical of a ferrimagnet with both low coercive-field and remanent magnetization. Below 46 K the magnetic behavior becomes unusual as already reported.^{20–22} The coercivity increases strongly and we notice the appearance of strong magnetic training and thermoremanent magnetization. At very low temperature the high-field susceptibility is unusually large. We shall describe all these phenomena in details in the following.

1. Coercive field

The temperature dependence of the coercive field H_c is shown in Fig. 2 where H_c has been measured

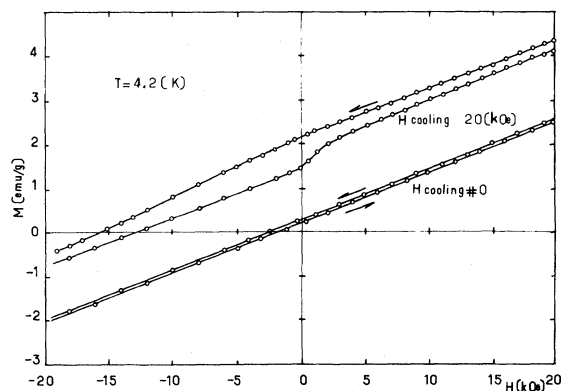


FIG. 4. Low-field magnetization loops at 4.2 K, respectively, obtained after (a) cooling the specimen in a zero field, and (b) cooling the specimen in a 20-kOe field.

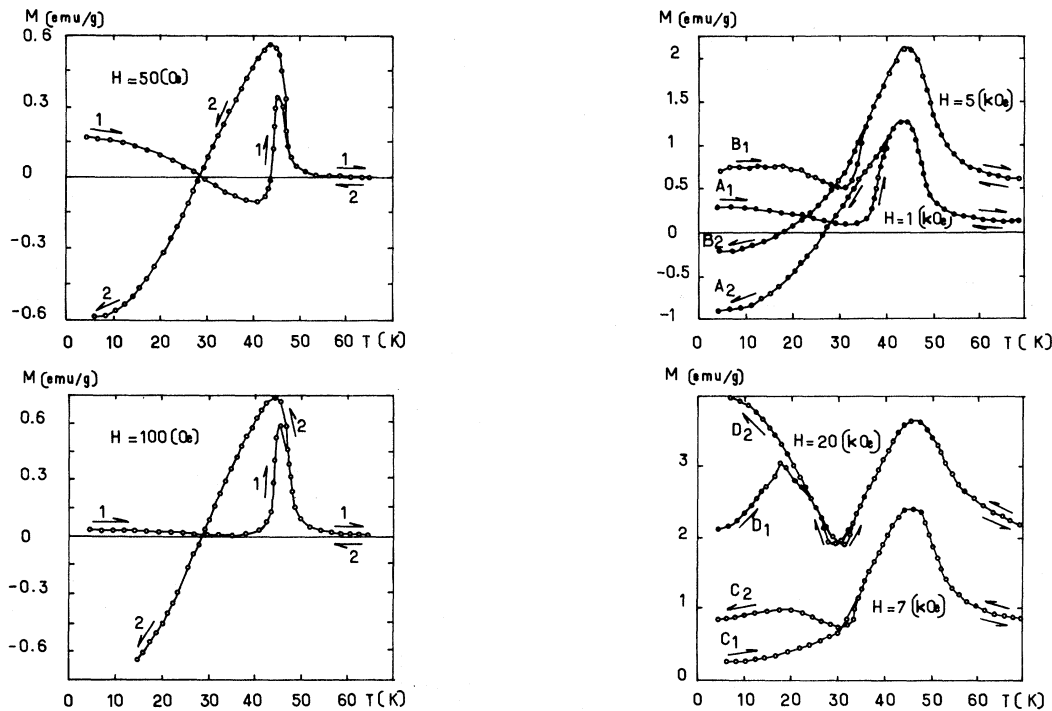


FIG. 5. Magnetization vs temperature for several applied fields: (1) zero-field-cooled specimen, (2) specimen cooled in the field.

by applying and removing a field of 20 kOe. The data need two comments. As we shall see later the collapse of H_c at 28 K is related to the compensation temperature where the bulk magnetizations of both sublattices balance each other. On the other hand, the decrease of the coercive field at low temperature arises from a lack of saturation of the sample in a 20-kOe field. We report in Fig. 3 the magnetization curve obtained in magnetic fields up to 150 kOe at 4.2 K, H_c is then 12 kOe, and strong irreversible magnetization processes are observed in fields up to 100 kOe. The coercive field, which is very small between 55 and 46 K, increases below 46 K if we disregard the singular behavior at 28 K.

2. Thermoremanent magnetization

Figure 4 shows the magnetization curves obtained after cooling the sample from temperatures larger than 55 K to 4.2 K, respectively, in a nearly zero field and in a 20-kOe field. The thermoremanent magnetization (2 emu/g) approaches the magnetization measured at 20 kOe when the sample is cooled in a zero field. The temperature

dependence of the thermoremanent magnetization may be illustrated with the help of the following procedure. The sample is cooled to 4.2 K in a nearly zero field from temperatures larger than 55 K. A given field is applied and the magnetization is recorded in increasing temperatures up to values larger than 55 K and then in decreasing temperatures. The results reported in Fig. 5 show the appearance of important thermoremanent magnetization below 46 K. Another striking feature is that the magnetization may lie in a direction opposite to the field in magnetic fields smaller than 7 kOe.

3. Magnetic training

Below 46 K the magnetization depends both on magnetic field and time. The time dependence of the magnetization is so important that it makes the reproducibility of the data very difficult. We have carried out two kinds of measurements. In the first kind the sample is cooled to a given temperature below 46 K in a 20-kOe magnetic field. The field is then removed and the time dependence of the thermoremanent magnetization is recorded. In the

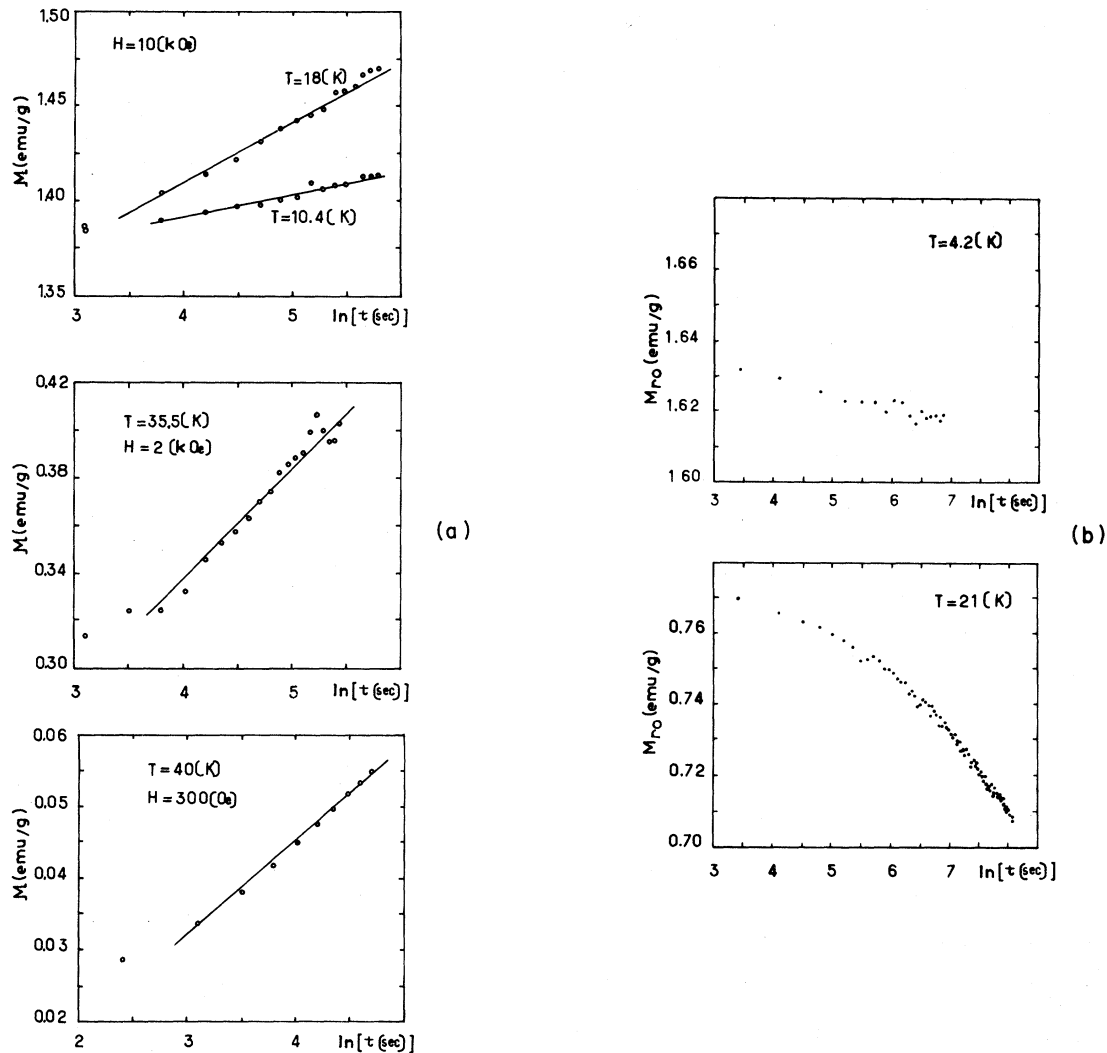


FIG. 6. Time dependence (a) of the magnetization after applying a given magnetic field and (b) of the remanent magnetization.

second kind of measurement the sample is cooled in a zero field and the magnetization is recorded after a given magnetic field has been applied. The variation of the magnetization depends on both temperature and strength of the field. A strong effect is observed in fields which become smaller as the temperature increases. The variations M of the magnetizations are plotted versus \ln (Fig. 6) for both kinds of measurements and an almost linear relation is observed.

4. High-field susceptibility

Another characteristic feature of Co_2TiO_4 is the lack of saturation in very high magnetic fields at

low temperature as shown in Fig. 3. In fact, the high-field magnetization approximately satisfies the following law at any temperature:

$$M = M_0 + \chi H. \quad (1)$$

The high-field susceptibility reported in Fig. 7 varies above 40 K as it does in any collinear ferrimagnetic structure and shows a singularity at 55 K. Below 40 K, χ strongly deviates from what may be expected for a collinear ferrimagnet where the high-field susceptibility arises from spin-wave excitations and then vanishes at low temperature. The results obtained in fields up to 20 kOe are certainly not significant at low temperature where the coercivity is very important. The low-temperature susceptibility

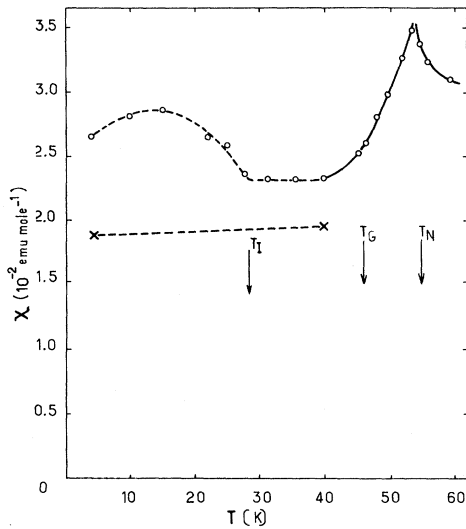


FIG. 7. High-field susceptibility vs temperature: (○) in a 20-kOe and (×) in a 150-kOe magnetic field.

obtained in fields up to 150 kOe where certainly the technical saturation is reached would seem to indicate that the excitations are not conventional spin waves below 46 K and suggests a transition temperature around 46 K. The lack of saturation at low temperature is also confirmed by the low value of $M_0 = 0.10\mu_B/\text{mole}$ estimated from (1) at 4.2 K, while a collinear spin configuration would yield $0.27\mu_B/\text{mole}$ from high-temperature data.

5. Compensation temperature

We have plotted in Fig. 8 the remanent magnetization obtained after applying and removing a field of 20 kOe. The remanent magnetization vanishes at

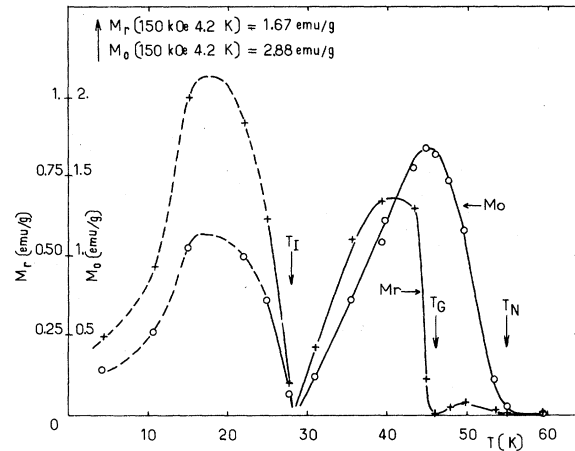


FIG. 8. Temperature dependence of the remanent magnetization M_r (+) and of the bulk magnetization M_0 (○) obtained in a 20-kOe magnetic field.

28 K as the result of the collapse of the bulk magnetization M_0 arising from the compensation of the average magnetizations of the A and B sublattices. This compensation temperature agrees with a long-range ferrimagnetic order.

B. Neutron-diffraction experiments

At 4.2 K the neutron-diffraction pattern (Fig. 9) shows magnetic reflections which are those of a collinear ferrimagnet. However, a careful examination near the (111) point of the reciprocal lattice shows that the peak is too large for a Bragg reflection and furthermore we notice the presence of a broad

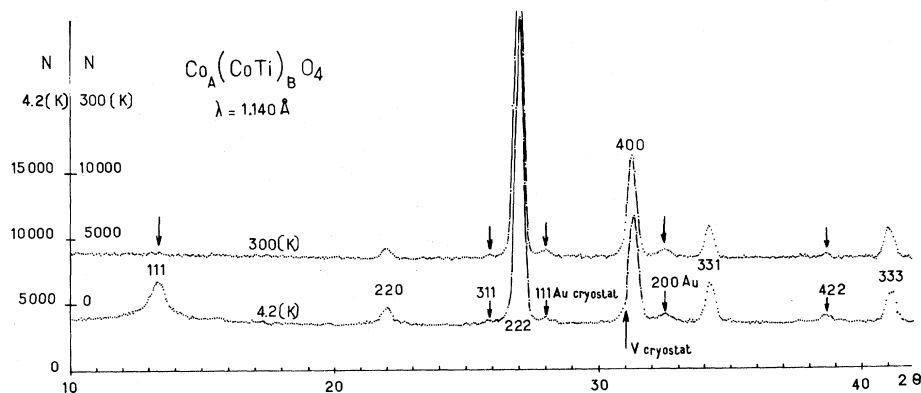


FIG. 9. Neutron-diffraction pattern, respectively, at 300 and 4.2 K.

liquid peak (Fig. 10). We report in Fig. 11 the temperature dependence of the intensity scattered in the (111) direction, and if the coherent scattering vanishes at 55 K, the diffuse scattering is still important at 105 K (Fig. 10). Such a behavior has already been observed in spiral structures^{26,27} and explained as paramagnetic diffuse scattering.²⁸ At low temperature a spiral structure would yield well-resolved Bragg reflections which are missing in our diffraction pattern; however, the enhancement of the diffusion near the (200) and (420) directions suggests a canted spin configuration at least on the *A* sublattice with middle-range correlations.

IV. DISCUSSION

The overall behavior of the Co_2TiO_4 compound is ferrimagnetic with a Néel temperature of 55 K. However, the unusually large value of the high-field susceptibility and the low value of M_0 at low temperature suggest a canted ground-state spin configuration. Besides an average longitudinal spin component yielding the superlattice reflections observed in the neutron-diffraction pattern, there must be a disordered transverse spin component which produces the strong diffuse neutron scattering around the (111) peak. One may add that thermoremanent magnetization and magnetic training are characteristic of disordered spin configurations. The sys-

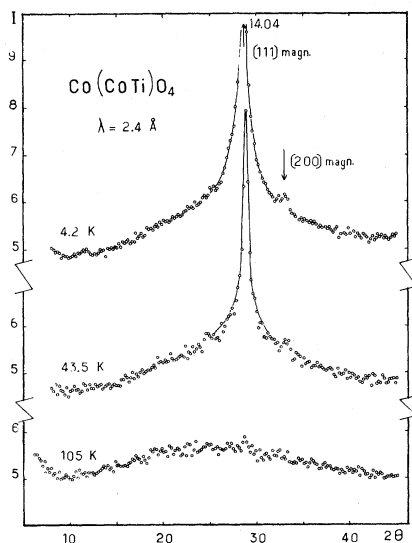


FIG. 10. Neutron-diffraction pattern showing the diffuse scattering around the (111) peak, respectively, at 4.2 and 105 K.

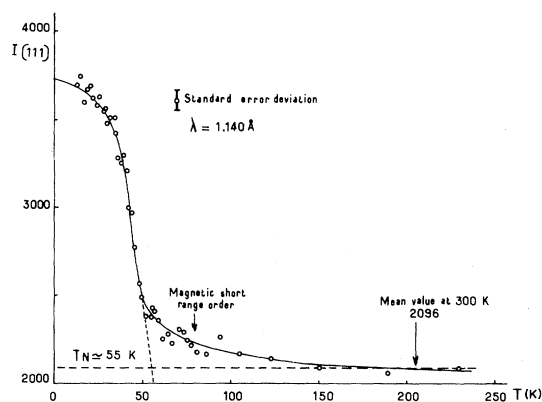


FIG. 11. Temperature dependence of the intensity of the (111) reflection.

tem consisting of a nonvanishing average longitudinal spin component and of a transverse spin-glass component, called "semi-spin-glass" by Villain,¹² results from the dilution of the magnetic ions in highly frustrated compounds. As a result of both dilution and frustration the spins may be locally canted²⁹ and it has been shown by Villain¹² that a canted local spin induces a long-range spin canting which decreases as a dipole field. The canted local spins (CLS) are then coupled through their "polarization clouds" even for low concentration in CLS. Villain has therefore predicted two transitions in a semi-spin-glass, the Néel temperature corresponding to the collapse of the longitudinal spin component and a second temperature T_G at which the transverse spin component freezes in. Below T_G all the features of a spin-glass must be observed. Owing to the similarities between our observations and the theoretical predictions we claim that the Co_2TiO_4 compound is a semi-spin-glass with $T_G = 46$ K.

The origin of the frustration producing the canting of the spins is not clear and cannot be inferred from the data. However, we would like to suggest two hypotheses. In the spinel structure, the *A-B* interactions are usually the strongest and the collinear spin configuration results. Nevertheless, canted structures may result from suitable intrasublattice interactions. If the hypothetical nondiluted system was collinear, the canting may only arise from the *A-A* interactions which are probably important for the Co^{2+} ions in tetrahedral coordination. In Co_3O_4 , where the cobalt ions in the *B* sites are in a low-spin state ($S=0$), the transition temperature is 40 K.³⁰ On the other hand, Co^{2+} is strongly anisotropic especially in the octahedral sites. Then the

presence of Ti^{4+} ions randomly distributed on the B sites may locally break the octahedral symmetry of the crystal field and produce a random anisotropy. Villain has only considered isotropic interactions but the extension of his theory to the anisotropic system leads to the same conclusions (see the Appendix).

In a spin-glass, the thermoremanent magnetization and the magnetic training result from the response of the spins to a magnetic field which is far from being well understood. In a semi-spin-glass, however, we suggest that thermoremanent magnetization and the magnetic training may be easily interpreted in the framework of the Néel theory of domain-wall motion.

As in any ferrimagnetic material, the crystal is split into magnetic domains separated by Bloch walls whose motion yields the main part of the magnetization in low fields. Following Néel³¹ the coercive field H_c increases as the mean-square value (msv) of the disordered transverse spin component and we may consider H_c as a measure of the canting of the spin configuration. The increase of the coercive field below 46 K then traduces the growing up of the spin-glass component. In the framework of Néel's theory, the collapse of H_c near the compensation temperature is related to the corresponding collapse of the msv of the spin-glass component taken over a macroscopic scale. That suggests a quasilocal collinearity of the spins which is consistent with the observation of the strong (200) and (420) reflections in the neutron-diffraction pattern which suggests middle-range correlations of the transverse spin components.

The magnetization curves shown in Fig. 4 may be understood if we assume that the magnetization approximatively follows a square loop bounded, respectively, by the bulk magnetization M_0 and by the coercive field H_c . In fields lower than H_c the virgin magnetization is always small. Consequently, above T_G where H_c is very small, the temperature dependence of the magnetization is that of M_0 . However, below T_G the magnetization must strongly depend on the strength of the magnetic field H with respect to the coercive field $H_c(T_I)$ at the compensation temperature, or more precisely on the ratio

$$r = H/H_c(T_I). \quad (2)$$

In the low fields and in increasing temperature the magnetization remains small as long as H is smaller than $H_c(T)$, i.e., up to T_G for r smaller than one or up to T_I for r larger than one. In decreasing

temperature the domain walls are pinned up at any temperature below T_G for r smaller than one and the resulting magnetization is M_0 between T_I and T_G and $-M_0$ below T_I . On the contrary, for r larger than one, the domain walls respond to the field near T_I and the magnetization always follows the bulk magnetization. This behavior is observed in fields up to 5 kOe. The departure from the above description of the curves plotted at 1 and 5 kOe in increasing temperature results from the high-field susceptibility which has not been taken into account.

The thermoremanent magnetization is also a result of the coercivity. The domain walls are pinned up in moderate fields at low temperature and the resulting magnetization is small. On the contrary, the domain walls are moving in the same field above T_G where the coercive field is small and a large magnetization is then observed as the sample is cooled at low temperature. The thermal hysteresis must decrease in increasing fields and almost vanishes in fields larger than the low-temperature coercive field. This is in agreement with the data. It has been shown by Néel³² that the excitation of spin waves modifies the transverse component of the magnetization and consequently produces a time-dependent coercivity. A time-dependent magnetization increasing as \ln must then be observed in any compound where the magnetization results from domain-wall motion. However, the magnitude of the phenomenon shows an almost exponential increase with the coercive field³³ and if our observations are relevant to the Néel theory it is not surprising that no magnetic training is observed above T_G .

V. CONCLUSION

The magnetic ground state of the Co_2TiO_4 compound may be described as the superposition of an average longitudinal ferrimagnetic component and of a transverse spin-glass component. As the temperature increases the canted spin configuration undergoes a transition to a collinear spin configuration at a well-defined temperature as does a helical structure in a nondiluted system. The ground-state spin configuration, called semi-spin-glass by Villain, may then be considered as a helical structure with a random pitch. At low temperature, all the usual features of a spin-glass are observed, but the presence of the average longitudinal spin component provides a simple interpretation for the high coercivity, thermoremanent magnetization, and magnet-

ic training. The origin of the canting cannot be inferred from the data, but sufficiently large A - A interactions or random anisotropy may be considered.

ACKNOWLEDGMENTS

The authors are indebted to Dr. J. Villain for enlightening discussions on the spin-glass problem and to Dr. J. Durand for critical reading of the manuscript. They acknowledge the assistance of Dr. P. Meriel (CEN—Saclay), Dr. P. Burllet, and Dr. P. Convert (ILL—Grenoble) in the neutron-diffraction experiments.

APPENDIX: COOPERATIVE EFFECT OF CANTED LOCAL STATE IN AN ANISOTROPIC SYSTEM

In the theory of Villain [Z. Phys. B **33**, 31 (1979), Secs. 4 and 5] the collective freezing of the transverse spin components at the spin-glass “transition” results from the long-range interactions between the CLS. As that interaction arises from the overlap of the transverse polarization “clouds” induced in the matrix by the CLS, cooperative freezing is then expected whatever the origin of the CLS may be. Local anisotropy effects are relevant to the Villain spin-glass model.

It is easily shown that the canting extends over the matrix in an anisotropic system whose Hamiltonian is

$$H = - \sum_{i,j} A_{ij}^{\alpha\beta} \vec{S}_i \cdot \vec{S}_j, \quad \alpha, \beta = x, y, z. \quad (\text{A1})$$

Let us assume a collinear ground state with the spins lying in the z direction. As in the ground state the spins are parallel to the molecular field and the following relations hold:

$$\lambda_i S_i^z = \sum_j A_{ij}^{\alpha z} S_j^z, \quad (\text{A2})$$

$$0 = \sum_j A_{ij}^{\alpha\alpha} S_j^z \quad (\alpha = x, y). \quad (\text{A3})$$

We now give the spin deviations \vec{s}_i from the ground-state configuration. The conservation of the spin modulus implies

$$2S_i^z s_i^z + \vec{s}_i^2 = 0, \quad (\text{A4})$$

and with (A1) to (A4) the energy is found to be

$$E = - \sum_{i,j} A_{ij}^{\alpha\beta} s_i^\alpha s_j^\beta + \sum_{j,\alpha} \lambda_j s_j^{\alpha^2}, \quad \alpha, \beta = x, y, z. \quad (\text{A5})$$

The equilibrium equations have the following form:

$$\lambda_i s_i^\alpha - \sum_{j,\beta} A_{j,\beta}^{\alpha\beta} s_j^\beta = 0, \quad (\text{A6})$$

which traduces the propagation of the canting in the matrix once the CLS have been given.

Equation (10) in Villain's article $\nabla^2 s(r) = 0$ may be easily recovered from (A6) and (A2) in the case of an isotropic ferromagnetic if the spin deviations are treated as a continuous field.

¹F. Scholl and K. Binder, Z. Phys. B **39**, 239 (1980).

²J. Hubsch, G. Gavoille, and J. Bolfa, J. Appl. Phys. **49**, 1363 (1978).

³Y. Ishikawa, S. Sato, and Y. Syono, J. Phys. Soc. Jpn. **31**, 452 (1971).

⁴P. W. Readman, W. O'Reilly, and S. K. Banerjee, Phys. Lett. **25A**, 446 (1967).

⁵R. Vanleerberghe, E. De Grave, R. E. Vandenberghe, and G. Robbrecht, J. Magn. Mater. **15-18**, 55 (1980).

⁶E. Hermon, D. J. Simkin, R. J. Haddad, and W. B. Muir, J. Phys. (Paris) Colloq. **C1**, C1-131 (1977).

⁷E. Hermon, D. J. Simkin, R. J. Haddad, and W. B. Muir, in *Magnetism and Magnetic Materials—1975 (Philadelphia)*, Proceedings of the 21st Annual Conference on Magnetism and Magnetic Materials, edited by J. J. Becker, G. H. Lander, and J. J. Rhyne (AIP, New York, 1976), p. 576.

⁸L. M. Corliss, J. M. Hastings, and F. G. Brockman,

Phys. Rev. **90**, 1013 (1953).

⁹E. De Grave, R. Vanleerberghe, C. Dauwe, J. De Sitter, and A. Govaert, J. Phys. (Paris) Colloq. **37**, C6-97 (1976).

¹⁰Our own measurements on Fe₂MgO₄-TiMg₂O₄.

¹¹G. A. Sawatzky, F. Van der Wonde, and A. H. Morrish, Phys. Rev. **187**, 747 (1969).

¹²J. Villain, Z. Phys. B **33**, 31 (1979).

¹³G. Toulouse, Commun. Phys. **2**, 115 (1977); J. Villain, J. Phys. C **10**, 1717 (1977); **11**, 745 (1978).

¹⁴P. W. Anderson, J. Less-Common Met. **62**, 291 (1978).

¹⁵B. Derrida, J. M. Maillard, J. Vannimenuis, and S. Kirkpatrick, J. Phys. Lett. **39**, L465 (1978).

¹⁶R. Rammal, R. Suchail, and R. Maynard, Solid State Commun. **32**, 487 (1979).

¹⁷H. Maletta and W. Felsch, Z. Phys. B **37**, 55 (1980).

¹⁸H. Maletta and W. Felsch, Phys. Rev. B **20**, 1245 (1979).

¹⁹K. Binder, W. Kinzel, H. Maletta, and D. Stauffer, J.

- Magn. Magn. Mater. 15-18, 180 (1980).
- ²⁰N. Sakamoto, J. Phys. Soc. Jpn. 17, 99 (1962).
- ²¹K. De Stropper, G. Robbrecht, and V. Brabers, C. R. Acad. Sci. Ser. B 277, 395 (1973).
- ²²K. De Stropper, C. Henriët-Iserentant, G. Robbrecht, and V. Brabers, C. R. Acad. Sci. Ser. B 277, 75 (1973).
- ²³F. A. Cotton and R. H. Holm, J. Am. Chem. Soc. 82, 2983 (1960); J. Chem. Phys. 31, 788 (1959).
- ²⁴J. Owen and J. H. M. Thornley, Rep. Prog. Phys. 29, 675 (1966).
- ²⁵F. Varret and F. Hartmann-Boutron, Ann. Phys. (N.Y.) 3, 157 (1968).
- ²⁶J. M. Hastings and L. M. Corliss, Phys. Rev. 126, 556 (1962).
- ²⁷N. Menyuk, K. Dwight, and A. Wold, J. Phys. (Paris) 25, 528 (1964).
- ²⁸T. A. Kaplan, H. E. Stanley, K. Dwight, and N. Menyuk, J. Appl. Phys. 36, 1129 (1965).
- ²⁹A. Rosencwaig, Can. J. Phys. 48, 2857 (1970).
- ³⁰W. L. Roth, J. Phys. Chem. Solids 25, 1 (1964).
- ³¹L. Néel, Ann. Univ. Grenoble 22, 299 (1946).
- ³²L. Néel, J. Phys. Rad. 11, 49 (1950); 12, 339 (1951).
- ³³J. C. Barbier, thesis, Grenoble (Masson, Paris, 1953).